

Treponema denticola Superoxide Reductase: In Vivo Role, in Vitro Reactivities, and a Novel [Fe(Cys)₄] Site

Jonathan D. Caranto,[‡] Linda L. Gebhardt,[§] Charles E. MacGowan,[§] Ronald J. Limberger,[§] and Donald M. Kurtz, Jr.*[‡]

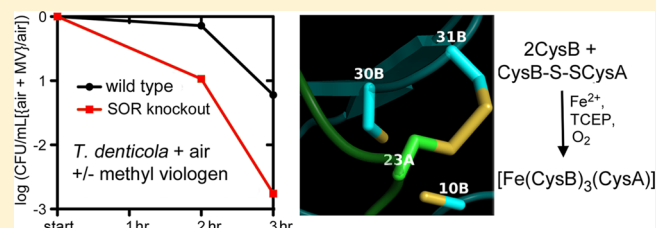
[‡]Department of Chemistry, University of Texas at San Antonio, San Antonio, Texas 78249, United States

[§]Wadsworth Center, New York State Department of Health, Albany, New York 12201, United States

Supporting Information

ABSTRACT: In vitro and in vivo results are presented demonstrating that superoxide reductase (SOR) from the air-sensitive oral spirochete, *Treponema denticola* (Td), is a principal enzymatic scavenger of superoxide in this organism. This SOR contains the characteristic non-heme [Fe(His)₄Cys] active sites. No other metal-binding domain has been annotated for Td SOR. However, we found that Td SOR also accommodates a [Fe(Cys)₄] site whose spectroscopic and redox properties resemble those in so-called 2Fe-SORs.

Spectroscopic comparisons of the wild type and engineered Cys → Ser variants indicate that three of the Cys ligands correspond to those in [Fe(Cys)₄] sites of “canonical” 2Fe-SORs, whereas the fourth Cys ligand residue has no counterpart in canonical 2Fe-SORs or in any other known [Fe(Cys)₄] protein. Structural modeling is consistent with iron ligation of the “noncanonical” Cys residue across subunit interfaces of the Td SOR homodimer. The Td SOR was isolated with only a small percentage of [Fe(Cys)₄] sites. However, quantitative formation of stable [Fe(Cys)₄] sites was readily achieved by exposing the as-isolated protein to an iron salt, a disulfide reducing agent and air. The disulfide/dithiol status and iron occupancy of the Td SOR [Fe(Cys)₄] sites could, thus, reflect intracellular redox status, particularly during periods of oxidative stress.

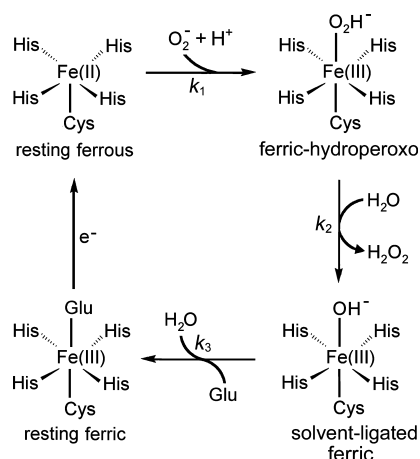


Superoxide reductases (SORs) are bacterial and archaeal oxidative stress protection enzymes associated with the “anaerobic lifestyle”.^{1–5} An extensive body of evidence has accumulated showing that SORs catalyze the one-electron reduction of superoxide to hydrogen peroxide at a nonheme [Fe(His)₄Cys] site according to the consensus mechanism shown in Scheme 1.^{1,4,6–8} This [Fe(His)₄Cys] site is a unique and defining feature of SORs and will hereafter be referred to as

the SOR site. The SOR site is structurally and functionally distinct from those in all known superoxide dismutases (SODs), the other major type of superoxide-scavenging enzymes. In fact, SORs show little or no SOD activity.^{5,9}

Various trivial names and acronyms have been applied in attempts to classify SORs.⁴ Based on homologies to well-characterized SORs, the majority of database sequences can be classified as either 1Fe- or 2Fe-SORs. The characterized 1Fe-SORs are homotetrameric, single-domain proteins and contain the SOR site as the only prosthetic group.¹⁰ The characterized 2Fe-SORs are homodimeric, as exemplified by the *Desulfoarculatus baarsii* (Db) 2Fe-SOR structure shown in Figure 1.¹¹ The C-terminal domain within each subunit of 2Fe-SORs contains the SOR site, which is essentially isostructural with that in 1Fe-SORs. The N-terminal domain of 2Fe-SORs contains an [Fe(Cys)₄] site,¹² which is often referred to as “Center I” to distinguish it from the SOR site. The structure of the Center I domains in all 2Fe-SORs that have been characterized up to now is distinct from the prototypical [Fe(Cys)₄] protein, rubredoxin, and is instead reminiscent of a small protein called desulfuredoxin.⁴ Center I in 2Fe-SORs was initially presumed to mediate intrasubunit electron transfer from redox partner proteins to the SOR site, but the published evidence does not

Scheme 1



Received: May 21, 2012

Revised: June 19, 2012

Published: June 20, 2012



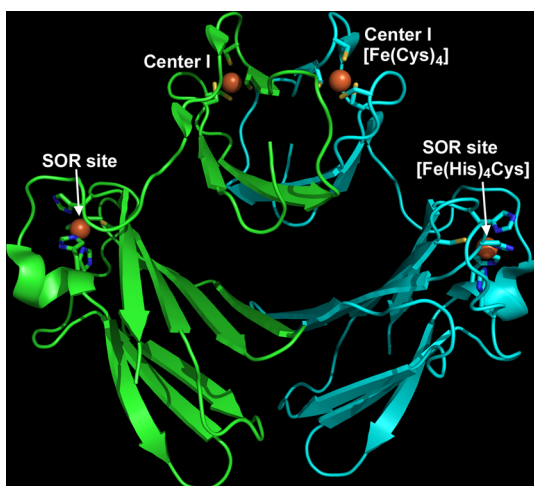


Figure 1. Protein backbone and iron site structures of the *D. baarsii* 2Fe-SOR homodimer (PDB ID 2J11). Protein backbone is shown in cartoon mode with the individual subunits colored green or cyan. Iron ligand residues are shown in stick mode, and iron atoms are depicted as orange spheres. Drawing was generated in PyMOL (Delano Scientific LLC).

support this function.⁴ In fact, disruption of the $[\text{Fe}(\text{Cys})_4]$ site in a 2Fe-SOR had no apparent effect on SOR activity either in vitro or in vivo.¹³

A third class (Class III) was proposed based on characterization of an SOR from the anaerobic spirochete, *Treponema pallidum* (Tp).^{14–16} Tp SOR has the two-domain structure and C-terminal SOR site characteristic of 2Fe-SORs. The N-terminal domain of Tp SOR, however, lacks three of the four Center I Cys residues (see Figure 2) and apparently binds no metal ion. Class III SORs were more recently proposed to include database sequences in which the N-terminal domains contain variable numbers (0, 1, 2, 3, 5, or 6) of Cys residues but no consensus metal binding sequence motif.^{12,a} Included in this expanded Class III is an uncharacterized SOR homologue from another spirochete, *Treponema denticola* (Td). The C-terminal region of the Td SOR sequence contains the $[\text{Fe}(\text{His})_4\text{Cys}]$ active site motif, whereas the N-terminal region is not annotated to contain a Center I or any other metal binding domain. However, as shown in Figure 2, three of five Cys residues in the N-terminal region align with Center I Cys ligand residues in “canonical” 2Fe-SORs.

T. denticola is a Gram-negative, motile, anaerobic spirochete.¹⁸ It is a normal constituent of the human oral microbiota

and is especially prominent in dental biofilms associated with chronic periodontitis.^{19,20} The periodontal environment is redox stressful for anaerobes, but the *T. denticola* genome does not contain open reading frames encoding recognizable SODs or catalases, which typically provide oxidative stress protection in aerobic bacteria.²¹ The *T. denticola* genome does, however, encode homologues of SOR and other proteins (e.g., rubrerythrin, peroxiredoxin, flavodiiron protein) associated with oxidative stress protection in many air-sensitive bacteria.^{22,23} The transcript for the putative SOR was reported to be upregulated upon exposure of *T. denticola* cultures to air.²⁴ Here we show that Td SOR exhibits the expected in vitro reactivity with superoxide at its SOR site and provide direct evidence for a superoxide scavenging function in vivo. We also show that Td SOR can accommodate $[\text{Fe}(\text{Cys})_4]$ sites in its Center I domains using a “noncanonical” Cys residue.

MATERIALS AND METHODS

Reagents. Reagents and buffers were the highest grades commercially available. All solutions were prepared using water purified with a Milli-Q ultrapurification system (Millipore) to a resistivity of 18.2 M Ω to minimize contamination by trace metal ions. Potassium hexachloroiridate(IV) and potassium superoxide were purchased from Sigma-Aldrich. Restriction enzymes were purchased from New England Biolabs.

Bacterial Strains and Culturing. *T. denticola* (ATCC 35405) was grown in new oral spirochete medium (NOS) with 10% heat-inactivated rabbit serum and 10 mg of cocarboxylase per mL at 36 °C in an anaerobic chamber (Coy Laboratory Products, Inc., Grass Lake, MI) with an atmosphere of 85% nitrogen, 5% carbon dioxide, and 10% hydrogen. For growth on semisolid media, 0.5% agarose was included with NOS (NOS agarose). *E. coli* DH5 α (Gibco BRL, Grand Island, NY) was used for most transformations and was grown aerobically in Luria–Bertani (LB) broth at 37 °C with shaking. Non-methylated plasmid DNA was prepared in *E. coli* SCS110 (Stratagene Corp., La Jolla, CA) for electroporation of *T. denticola*.

Insertional Inactivation of the Td SOR Gene. The SOR gene (TDE1754) was inactivated by insertion of an erythromycin resistance (*erm*) cassette based on a published protocol.¹⁸ Details are described in the Supporting Information. The resulting *T. denticola* 35405 strain containing the insertional inactivated TDE1754 gene is hereafter referred to as 1754M.

Oxidative Stress Phenotypes of Wild Type and 1754M *T. denticola* 35405 Strains. Dioxygen tolerance was assessed

	1		70
Db	MPERLQVYK C .EV C GNIVEVLNGGIGELV CC NQDMKLSENTVDA AK EHVPVIEKIDGGYKVKVGA VAH		
Tp	MGRELSFFLQKESAGFFLGMDAPAGSS VA CGSEVLRAVPVGTVD AAK EHIPVVEVHGHEVKVKVGS VAH		
Td	MSKEISFFL C KEKGTIIGID CC PD AEVS CGEKLSAVKIGSVDA AK EHVPVVEVNGNTVKVKVGS VAH		
Tph	MSKTIDFFL C NKGIGTFIALD AK DAEV S CGEKLA AVKIGSVDA AK EH VPVIEVHGTTVTVKIGS AEH		
	71		129
Db	PMEEK HY IQWIELLADDKCYTQFLKPGQAP EA VF LIEA AKVV..AREY CNI HGHWA EN		
Tp	PMTPE HY IAWVCLKTRKGIQLKELPVDGAPEVTFALTADDQVLEAYEF CNL HGVWSG K		
Td	PMTE EH HIAWVCLKTEKGLQFKELAVTGAP EV FS LT SDDKVIEAYEF CNL HGVWSG K		
Tph	PMTPE EH HIAWVCLKTEKGLQFKELPVDGKPEVEFSITADDKVIEAYEF CNL HGVWSG K		

Figure 2. Amino acid sequence alignment of *D. baarsii* (Db) 2Fe-SOR, *T. pallidum* (Tp) SOR, and putative SORs from *T. denticola* (Td) and *T. phagedenis* (Tph) (NCBI Genbank accession numbers: ADK85415 (Db), ADD72914 (Tp), AAS12269 (Td), and ZP_08038067 (Tph)). “Canonical” Center I Cys residues are highlighted in red, and SOR site ligand residues are highlighted in blue. “Noncanonical” Cys residues are yellow-highlighted. Sequences were aligned using the Multalin version 5.4.1 server (<http://multalin.toulouse.inra.fr/multalin/multalin.html>).

by exposing either liquid cultures or 0.5% agar-plated strains to air (~20% (v/v) O₂). Air-exposed liquid cultures contained NOS minus cysteine and thioglycollate, whereas all NOS agarose plates contained the usual amounts of cysteine and thioglycollate since these strains would not grow well on plates lacking these reducing agents. For air exposures on plates, liquid cultures were grown to an OD₅₅₀ of 0.2 in NOS (minus cysteine and thioglycollate) in the anaerobic chamber. The cultures were serially diluted and plated on NOS agarose in the anaerobic chamber (six sets of serial dilutions). The plates (except for time 0) were removed from the anaerobic chamber and placed in air at 37 °C. At hourly intervals subsets of the plates were returned to the anaerobic chamber. Colonies were counted after 9 days anaerobic incubation at 36 °C, from which colony forming units per mL of culture (CFU/mL) were determined. For liquid-media “single-dose” air exposures, cultures (5 mL in 10 mL tubes) were grown at 36 °C to an OD₅₅₀ of 0.1–0.2 in the anaerobic chamber. 500 µL volumes of these cultures were diluted with 5 mL of air-saturated NOS (no cysteine or thioglycollate) that had been separately transferred to the anaerobic chamber. These diluted cultures were then overlaid with 1 mL of mineral oil and incubated at 36 °C. At set times following these dilutions samples were serially diluted and plated on NOS agarose in the anaerobic chamber. Colonies were counted after 9 days incubation at 36 °C. In order to assess the effect of methyl viologen (MV) on air-exposed cultures, a variation of a previously described procedure²⁵ was used. Thus, for both the wild type and 1754M strains, duplicate 45 mL cultures (in NOS minus cysteine and thioglycollate) in 250 mL flasks were grown to an OD₅₅₀ of ~0.2 in the anaerobic chamber. To one culture in each duplicate set was added MV to a final concentration of 100 µM. After removing samples for the time zero/anaerobic controls, the flasks were removed from the anaerobic chamber and shaken at 100 rpm in an aerobic incubator at 36 °C. Samples of each culture were removed at hourly intervals, serially diluted, and plated on NOS agarose in the anaerobic chamber. CFU/mL were determined after 9 days of incubation at 36 °C.

Cloning and Mutagenesis of the Td SOR Gene. The Td SOR gene (locus tag TDE1754) was amplified from genomic DNA isolated from *T. denticola* strain 35405.¹⁸ The purified PCR product was cloned into pCR2.1TOPO (Invitrogen) and then subcloned into the *NcoI/BamHI* multiple-cloning restriction sites of the *E. coli* expression vector, pKB6H, using the In-Fusion PCR Cloning System (Clontech). pKB6H (kindly provided by P. John Hart) is derived from pKM265^{26,27} and encodes an additional N-terminal amino acid sequence, MDHHHHHHHHASENLYFQGA, containing a 6x-His tag followed by a tobacco etch virus protease cleavage site. (The plasmid map is contained in Figure S3 of the Supporting Information.) The Center I Cys → Ser variant plasmids were constructed as described in the Supporting Information. Nucleotide sequences of the wild type and variant Td SOR genes in pKB6H were confirmed by sequencing at the University of Texas Health Science Center San Antonio Nucleic Acids Core Facility.

Overexpression, Isolation, and Purification of Td SOR. pKB6H containing either the wild type or Center I Cys → Ser variant Td SOR genes were heat-shock transformed into *E. coli* BL21 (DE3). The transformed cells were plated on agar containing Luria–Bertani (LB) medium supplemented with 100 mg/L ampicillin (LB/amp). Selected colonies were used to inoculate 30 mL volumes of LB/amp liquid medium. Following

overnight incubation with shaking at 37 °C, these 30 mL cultures were used to inoculate 1 L volumes of LB/amp, which were then incubated with shaking at 37 °C. When the 1 L cultures’ ODs reached 0.6–1.0, Td SOR overexpression was induced by addition of 100 mg/L isopropyl-β-D-thiogalactoside. After a further 4 h incubation at 37 °C with shaking, the cells were harvested by centrifugation and lysed by sonication in 50 mM MOPS, 250 mM NaCl, pH 7.3. The cell lysates were clarified by centrifugation, and the supernatants were adsorbed onto a 10 mL column containing Talon Cobalt resin (Clontech). The column was washed with 50 mM MOPS 250 mM NaCl, pH 7.3, and the His-tagged proteins were eluted with 50 mM MOPS, 250 mM NaCl, 250 mM imidazole pH 7.3. Imidazole and salt were removed from the proteins by multiple wash/concentration cycles using 50 mM MOPS, pH 7.3 in 10 000 molecular weight cutoff Amicon concentrators (Millipore). The purified proteins were stored at –80 °C.

Td SOR Antibodies and Western Blotting. Antisera against purified recombinant Td SOR (without the His tag) were raised in rabbits (Pacific Immunology Corp). Western blotting using the rabbit antiserum followed a standard procedure.²⁸

Iron/Protein Mole Ratios. Protein concentrations were determined via the bicinchoninic acid assay (Pierce) using bovine serum albumin as the standard. Iron concentrations were determined via a standard ferrozine assay.²⁹

Native Protein Size and Homogeneity. Native protein molecular weights were determined using size exclusion chromatography on a Superose 6 10/30 column (GE Healthcare) eluting at 0.5 mL/min with 30 mM MOPS pH 7.3 + 0.5 M NaCl. The column was calibrated using protein standards (Sigma).

Iron Enrichment of Recombinant Td SOR. Anaerobic manipulations were carried out as described in the Spectroscopy section. Either wild type or Cys → Ser variant Td SORs were anaerobically incubated for 1 h with 5 equiv of tris(2-carboxyethyl)phosphine (TCEP) in deoxygenated 50 mM MOPS, pH 7.3. The protein was then anaerobically treated with 2 equiv per protein monomer of ferrous iron by addition of a small volume of a concentrated stock ferrous ammonium sulfate hexahydrate solution in water. The iron-treated protein solution was then exposed to air, which resulted in the solution color changing to a darker red. Excess iron and TCEP were washed from the protein with air-saturated 50 mM MOPS, pH 7.3, via multiple dilution/concentration cycles in an Amicon centrifugal filter (Millipore).

Redox Manipulations of the Td SOR Iron Sites. Ferric Center I in the iron-enriched wild type Td SOR (in which the SOR sites are ferrous) was reduced anaerobically with 0.5 mol equiv per protein monomer of sodium dithionite. The ferric SOR site in either the as-isolated (containing apo Center I) or iron-enriched (containing ferric Center I) proteins was prepared by oxidation of the ferrous SOR site with 1.5 mol equiv of K₂IrCl₆. Enzymatic reduction of the SOR iron sites used NADH:rubredoxin oxidoreductase (NROR) and rubredoxin (Rd), both from *Thermotoga maritima*, which were obtained as previously described.³⁰ Rates of enzymatic reduction of the ferric Center I and SOR sites were measured using a procedure analogous to that described for *Desulfovibrio vulgaris* 2Fe-SOR.³¹ More experimental details are provided in the text and figure legends.

Spectroscopy. UV–vis absorption spectra were obtained on Ocean Optics USB 2000 spectrophotometers. For anaerobic

conditions spectra were obtained in a Vacuum Atmospheres Co. anaerobic chamber and/or in rubber septum/screw-capped quartz cuvettes to which reagents were added via gastight syringes.

Stopped-Flow Spectrophotometry. Stopped-flow spectrophotometry of the reaction of superoxide with Td SOR was performed as described previously.⁶ Briefly, the method consists of stopped-flow mixing 1 volume of a concentrated potassium superoxide solution in 0.1 M NaOH against 10 volumes of a well-buffered anaerobic SOR solution. More experimental details are provided in the figure legends. Rate constants were determined by global component spectral fits using the Pro-K software package (Applied Photophysics Ltd.) and are averages and standard deviations from 3 to 5 replicate determinations.

RESULTS AND DISCUSSION

In Vivo Role of Td SOR. Western blotting of anaerobically grown *T. denticola* cell extracts using antibodies raised against purified recombinant Td SOR (no His tag) confirmed that the anaerobically grown wild type *T. denticola* 35405 strain expresses Td SOR, whereas no SOR could be detected in the derived 1754M strain containing the insertionally inactivated Td SOR gene at the same total protein loading (see Figure S4 in Supporting Information). As expected, the wild type *T. denticola* was found to be air-sensitive in NOS minus thiol reducing agents. Anaerobically plated samples withdrawn from liquid cultures during their rapid shaking (270 ppm) in air showed no colony forming units after ~3 h of air exposure. Under the same conditions the 1754M strain became nonviable after ~2 h (data not shown). Alternative methods were explored in order to obtain more quantitative evidence for relative air sensitivities of the wild type vs 1754M strains. As shown in Figure 3 (top panel), the 1754M strain is significantly more air-sensitive than the wild type strain on NOS agarose plates exposed to air. A more dramatic differential sensitivity was observed when liquid cultures were diluted with a “single dose” of air-saturated NOS (minus thiol reducing agents) in an anaerobic chamber (Figure 3, bottom panel). Figure 4 shows that when liquid culture flasks were shaken in air, the 1754M strain was significantly more sensitive to methyl viologen (MV). MV is known to increase the superoxide flux in aerobically grown bacterial cells.²⁵ These results clearly support a role for Td SOR in oxidative stress protection of O₂-exposed *T. denticola* 35405, and, more specifically, in superoxide scavenging.

Physical and Spectroscopic Characterizations of Recombinant As-Isolated Td SOR. In order to avoid the extra TeV protease cleavage step, we used the His-tagged protein, purified as described in Materials and Methods, for the in vitro results reported here. We found that the Td SOR without the His tag and/or the His-tagged protein purified by ion-exchange chromatography behaved identically to the tagged protein purified by metal chelate affinity chromatography. The as-isolated recombinant Td SOR reproducibly contained ~0.9 Fe/protein monomer (see Table 1). Analytical size exclusion chromatography showed that, under nondenaturing conditions, the Td SOR is homodimeric. The concentrated (millimolar) as-isolated Td SOR was reddish in color. As shown in Figure 5, treatment of the as-isolated Td SOR with hexachloroiridate(IV) (or, as described below, superoxide) resulted in development of an absorption feature with $\lambda_{\text{max}} \sim 645$ nm characteristic of the ferric SOR site in which a glutamate ligand from a flexible loop

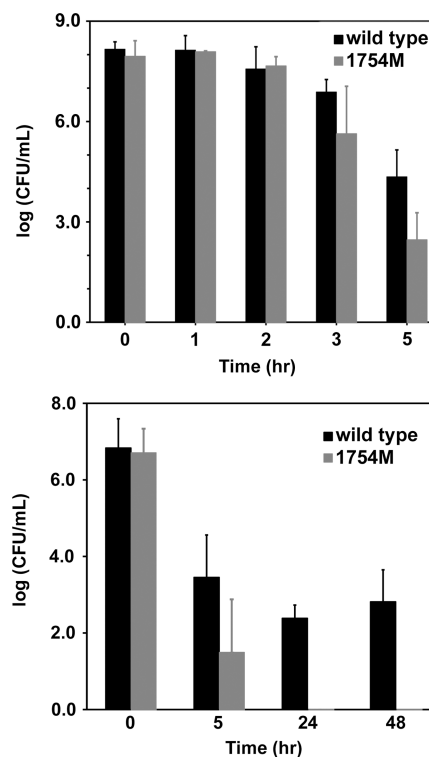


Figure 3. Air sensitivity of *T. denticola* 35405 wild type and 1754M strains on plates (top panel) and in liquid cultures (bottom panel). Top panel: strains on NOS agarose plates were exposed to air for the indicated time periods, the plates were returned to the anaerobic chamber, incubated at 36 °C, and colonies were counted after 9 days. Bottom panel: anaerobic liquid cultures were diluted 10-fold (v/v) with air-saturated NOS (minus cysteine and thioglycollate), the surfaces were layered with mineral oil, and the cultures were incubated at 37 °C in the anaerobic chamber. At the indicated times samples were removed, serially diluted, and plated on NOS agarose. For both the plate and liquid-culture air exposure experiments, CFU/mL were determined after 9 days of anaerobic plate incubation, and error bars represent standard deviations for at least three platings. For the liquid culture air exposures, no viable 1754M cells were detectable at 24 and 48 h.

on the protein is added trans to the Cys ligand (see Scheme 1). Since the ferrous SOR site in other SORs shows no electronic transitions in the visible region,^{32,33} we infer that the as-isolated Td SOR contains an air-stable ferrous SOR site. This redox behavior is characteristic of SORs and is consistent with the relatively positive ferric/ferrous reduction potentials (~300 mV vs NHE at pH 7) of SOR sites.^{2,4,13}

Iron Enrichment of Td SOR Center I. Iron enrichment of Td SOR to ~2 Fe/protein monomer (see Table 1) was reproducibly achieved by addition of a modest excess of ferrous salt and TCEP to anaerobic solutions of the as-isolated Td SOR followed by exposure to air and removal of excess reagents. The iron-enriched protein solution showed a greatly enhanced reddish color due to a large increase in the absorption feature with $\lambda_{\text{max}} \sim 460$ nm ($\epsilon_{460 \text{ nm}} = 4400 \text{ M}^{-1} \text{ cm}^{-1}$) and shoulder at ~525 nm (see Figure 5). This absorption spectrum of the iron-enriched protein resembles those of other 2Fe-SORs containing ferric Center I and ferrous SOR sites.³³ We, therefore, associate the 460 nm absorption feature with a ferric Center I [Fe(Cys)₄] site in Td SOR. Neither iron incorporation nor the enhanced 460 nm absorption occurred when TCEP was omitted during the iron enrichment but were stable following removal of

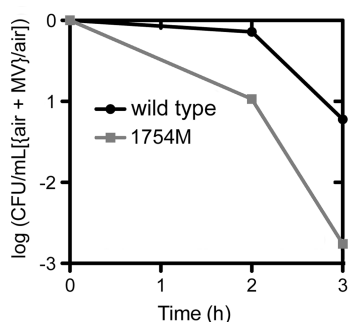


Figure 4. Differential air sensitivity of *T. denticola* 35405 wild type and 1754M strains in liquid cultures (NOS minus cysteine and thioglycollate) with vs without MV. Parallel sets of flask cultures containing either no MV or 100 μ M MV were shaken while exposed to air at 36 °C. At the indicated times samples were removed from each culture, transferred to the anaerobic chamber, serially diluted, plated on NOS agarose, and incubated in at 36 °C. Colonies were counted after 9 days. For each time point the ratio of CFU/mL obtained for the cultures containing MV divided by the CFU/mL for the cultures without added MV was calculated, and the log values of these ratios are plotted. Data points are the averages from three experiments. The 4 h data are not plotted since no viable 1754M cells were detected.

Table 1. Iron Contents of Td SOR Wild Type and Cys \rightarrow Ser Variants^a

protein	as-isolated	Fe-enriched
wild type	0.9	1.8
C10S	1.0	1.7
C22S	1.1	2.5
C23S	1.0	0.8
C30S	1.2	1.7
C31S	1.1	1.6

^aIn mol Fe/mol protein monomer, all values within a standard deviation of $\pm 10\%$.

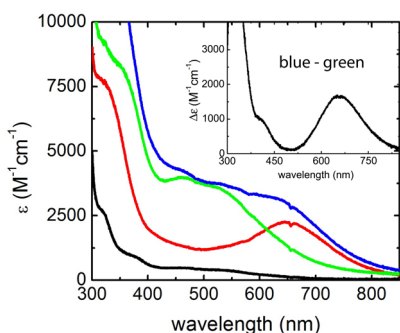


Figure 5. UV-vis absorption spectra of as-isolated (~ 1 Fe/protein monomer) and iron-enriched (~ 1.8 Fe/protein monomer) wild type Td SOR. Black trace: as-isolated; red trace: as-isolated + K_2IrCl_6 ; green trace: iron-enriched; blue trace: iron-enriched + K_2IrCl_6 . Inset shows blue trace – green trace difference spectrum. All samples were 100 μ M protein (monomer equivalent) in 50 mM MOPS, pH 7.3. The extinction coefficient axis is per protein monomer.

TCEP (see below). This observation indicates that formation of ferric Center I requires reduction of disulfide bonds.

Comparative Redox Properties of the Td SOR Iron Sites. As judged by UV-vis absorption spectra, the ferric Center I of Td SOR was stable for several days under anaerobic conditions at room temperature but gradually decayed over the same time period under aerobic conditions. The presence of

TCEP slowed the aerobic spectral decay, indicating that the decay reflects disulfide formation. The ferric Center I was not reducible by ascorbate even under anaerobic conditions, whereas the ferric SOR site was rapidly reduced by ascorbate (data not shown). Both the ferric Center I and the ferric SOR site could be reduced by stoichiometric sodium dithionite under anaerobic conditions. The reduced Center I reoxidized to the ferric form upon exposure to air, whereas the ferrous SOR site was air stable. These comparative redox behaviors qualitatively indicate that the Td SOR Center I has a significantly lower ferric/ferrous reduction potential than that of the SOR site. These redox properties parallel those of the corresponding iron centers in “canonical” 2Fe-SORs.⁴

Characterization of Center I Cys \rightarrow Ser Variants. The five Cys residues in the Center I domain of Td SOR (see Figure 2) were individually changed to Ser. Iron contents of the variants, both as-isolated and after the iron enrichment treatment, are listed in Table 1. UV-vis absorption spectra of the variants after the iron enrichment treatment are shown in Figure 6. The iron-enriched C22S variant contains slightly

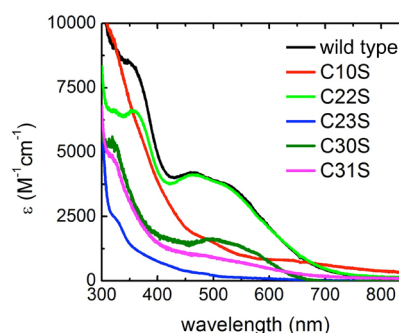


Figure 6. UV-vis absorption spectra wild type and Cys \rightarrow Ser variant Td SORs after the iron enrichment procedure. All samples were 100 microM (monomer equivalent) Td SOR in 50 mM MOPS, pH 7.3. Spectra were obtained under an aerobic atmosphere. The extinction coefficient axis is per protein monomer.

more than 2Fe/monomer, and its UV-vis absorption spectrum is essentially identical to that of the iron-enriched (~ 2 Fe/monomer) wild type protein in both shape and intensity. Since the wild type visible absorption spectrum is dominated by that of ferric Center I, C22S must quantitatively retain the wild type $[Fe(Cys)_4]$ site. The spectra of the other four variants following the iron enrichment procedure all show clear differences from that of the iron-enriched wild type protein. These differences are logically attributed to little or no iron enrichment in the C23S variant and substitution of a Ser or solvent in place of a Cys ligand in ferric Center I of the C10S, C30S, and C31S variants.^{34–36} The singular lack of iron enrichment in the C23S variant highlights the essential role of the noncanonical C23 in stabilizing the ferric Center I in Td SOR.

Reactions of Td SOR with Superoxide. Reactions of the Td SOR iron centers with superoxide were examined using our spectrophotometric stopped-flow methodology previously developed for a “canonical” 2Fe-SOR.⁶ Difference spectra were used to remove the contribution of the ferric Center I, which showed no apparent reaction with superoxide. Our stopped-flow results can be understood by referring to Scheme 1. In the case of *D. vulgaris* 2Fe-SOR, stopped-flow mixing of the protein containing ferric Center I and ferrous SOR site resulted in accumulation of a UV-vis absorption spectrum with

$\lambda_{\text{max}} \sim 600$ nm within the mixing dead time (~ 2 ms). Pulse radiolysis experiments had previously assigned this spectrum to a ferric–hydroperoxo SOR site resulting from diffusion-controlled reaction of the resting ferrous site with superoxide (k_1 in Scheme 1).³³ This stopped-flow “dead time” intermediate then smoothly decayed in a first-order process (~ 50 s^{−1}) to the “resting”, glutamate-ligated ferric SOR site with its characteristic 645 nm absorption.⁶ Detailed kinetics studies on the *D. vulgaris* 2Fe-SOR indicated that the apparent absence of the solvent-ligated species shown in Scheme 1 could be attributed to $k_3 \gg k_2$.⁶ As shown in Figure 7, we observed this same “ $k_3 \gg k_2$ ” spectral time course, manifested by the clean isosbestic points, for both as-isolated and iron-enriched wild type Td SOR. The $k_{\text{obs}} (\cong k_2)$ for decay of the 600 nm dead-time intermediate to resting ferric was 60 ± 4 s^{−1} for the as-isolated and 50 ± 4 s^{−1} for the iron-enriched Td SOR. Iron occupancy

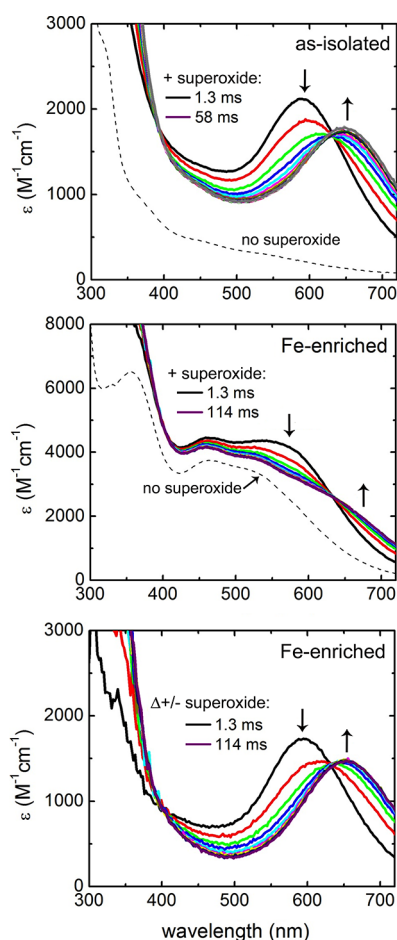


Figure 7. Stopped-flow spectral time courses of wild type Td SOR reactions with superoxide. Top panel: as-isolated; middle and bottom panels: iron-enriched. Conditions after mixing: 145 μM (monomer equivalent) iron-enriched Td SOR in 250 mM MOPS, pH 7.3, 2 mM DTPA, 2 mM KO_2 (nominal) at 4 °C. The individual spectral traces (differentiated by colors) were obtained in ~ 6 ms increments between the indicated initial and final times following the mixing dead time. Vertical arrows represent directions of absorbance changes with time. The dashed traces exemplify time courses for control experiments using the same protein samples, but omitting superoxide. The $\Delta\epsilon$ superoxide time course in the bottom panel represents the [+superoxide minus no superoxide] difference absorption spectra obtained from the spectral traces in the middle panel.

of Center I in Td SOR, thus, appears to have no significant effect on the reaction of superoxide with the SOR site.

Enzymatic Reduction of Td SOR Iron Sites. The all-ferric form of iron-enriched Td SOR was used to test relative rates of reduction of the Center I and SOR site irons by a reconstituted enzymatic system used previously to measure SOR activities in vitro.^{4,13,31,38,39} This system transfers reducing equivalents from NADH to the SOR iron sites via a generic NADH:rubredoxin oxidoreductase (NROR) and rubredoxin (Rd), the latter serving as the proximal electron donor to the SOR. This electron transport chain likely reflects the reductive portion of an intracellular SOR turnover pathway.^{4,31} For these studies the all-ferric form of iron-enriched Td SOR was prepared by oxidation with a modest excess of potassium hexachloroiridate(IV). As shown in Figure 8, the SOR site of Td SOR is reduced by the NADH/NROR/Rd system on the stopped-flow time scale (~ 1 s for complete reduction) and at similar rates whether or not Center I is occupied by iron. The

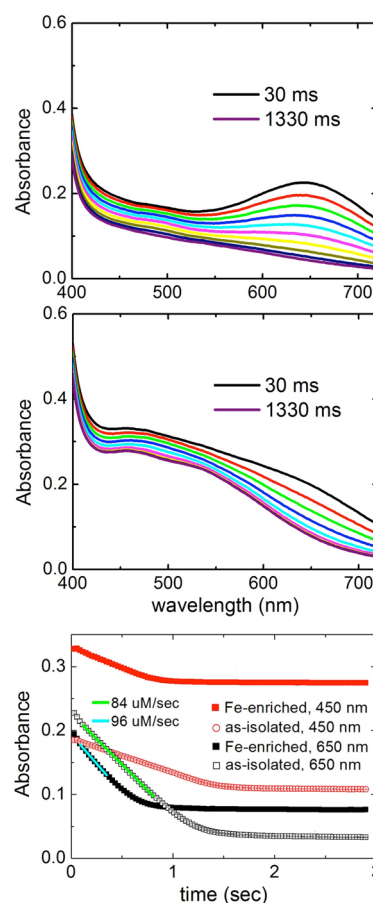


Figure 8. Stopped-flow spectral time courses for reduction of as-isolated (top panel) or iron-enriched (middle panel) Td SOR by NADH/NROR/Rd. An anaerobic solution of K_2IrCl_6 -oxidized Td SOR containing a 5-fold molar excess of NADH over protein monomer in one syringe was stopped-flow mixed, 1:1 (v/v), with an anaerobic solution of NROR/Rd and slight excess of NADH in the other syringe in 50 mM MOPS, pH 7.3, at room temperature. Concentrations after mixing: 145 μM (monomer equivalent) SOR, 725 μM NADH, 900 nM NROR, 4.5 μM Rd. Individual spectral traces between the indicated initial and final times after the mixing dead time are differentiated by colors. Bottom panel shows single wavelength time courses obtained from the corresponding spectra in the upper and middle panels.

ferric Center I, on the other hand, is not detectably reduced on this time scale. Figure 9, in fact, shows that ferric Center I is

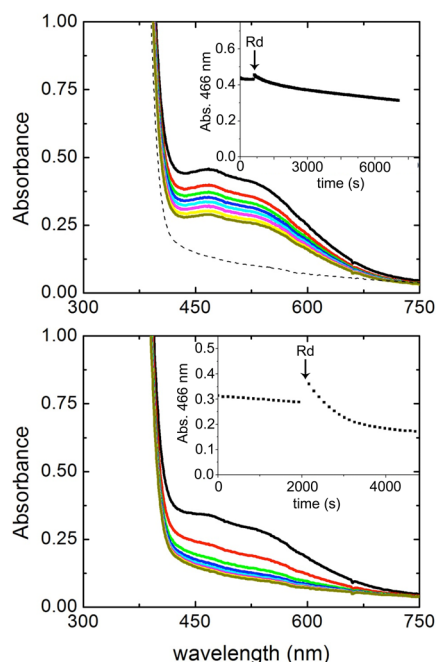


Figure 9. Manual mixing spectral time course of enzymatic Center I reduction in Fe-enriched Td SOR in 50 mM MOPS, pH 7.3, at room temperature under anaerobic conditions. Concentrations after mixing: 200 μ M (monomer equivalent) Fe-enriched Td SOR, 1 mM NADH, 5 μ M (upper panel) or 20 μ M (lower panel) Rd, and 1 μ M NROR. The highest intensity spectra (black traces) in each panel were obtained immediately after addition of Rd. Subsequent spectra were obtained at 1200 s intervals and are differentiated by colors. Insets contain the corresponding 466 nm absorbance vs time traces. For comparison, the dashed spectrum in the top panel is of fully reduced protein.

reduced ~ 3 orders of magnitude more slowly than is the ferric SOR site by the enzymatic system. Little or no reduction of either the ferric Center I or the ferric SOR site was observed when Rd was omitted from the enzymatic reduction system. These results parallel those for other 2Fe-SORs.^{4,13,31,38} Based on our previous analysis of the steady-state SOR catalytic cycle,³⁸ these results indicate that direct reduction of the ferric SOR site by the enzymatic system is kinetically competent to support catalytic reduction of superoxide without participation of Center I in Td SOR.

Homology Structural Modeling. Homology structural models of Td SOR were generated using the SWISS-MODEL server (<http://swissmodel.expasy.org/>).⁴⁰ In the automated mode the server selected the Tp SOR homodimer crystal structure as template, based on sequence homology. The Td SOR homodimer structure depicted in Figure 10 was drawn directly from the SWISS-MODEL-generated coordinates. Each subunit of the Td SOR model contains two domains. The C-terminal domain contains the expected SOR site iron ligand residues (blue-highlighted in Figure 2) at positions overlapping the corresponding residues in the Tp SOR template structure. Since the iron atoms were not modeled by the server, the coordinates of the SOR site irons from the template Tp SOR structure are superimposed onto the Td SOR structure shown in Figure 10. The resulting SOR site in the model is essentially isostructural with that in Tp SOR. The N-terminal domain of

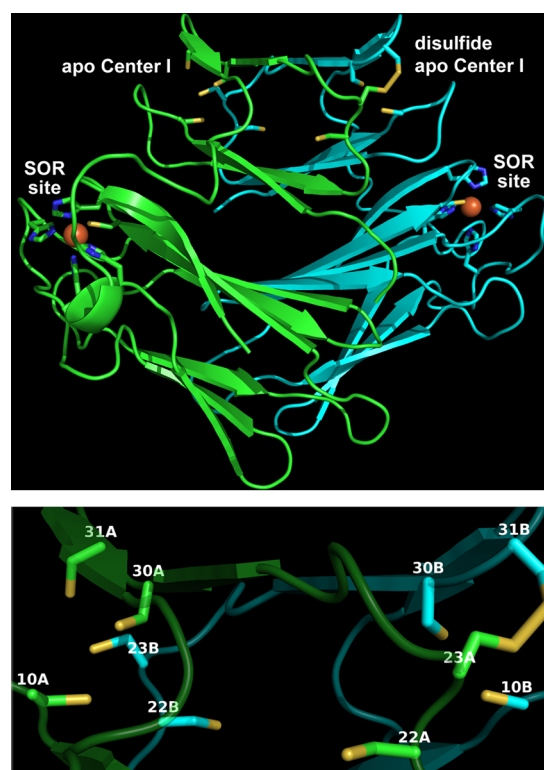


Figure 10. Td SOR structural model generated by SWISS-MODEL using the Tp SOR structure (PDB ID 1Y07) as template. The top panel shows the entire homodimer structure, and the bottom panel shows a close-up view of the two tetracysteine clusters in the Center I domains, one of which contains a disulfide. Protein backbone is shown in cartoon mode with individual subunits of the homodimer colored either green or cyan. SOR site residues and Center I domain Cys residues are shown in stick mode. Iron atom positions from the 1Y07 coordinates are shown as orange spheres. In the bottom panel the Center I Cys residues of the Td SOR model are labeled by sequence number and letter designating their occurrence in individual subunits, A or B, of the homodimer. Images were generated in PyMOL (Delano Scientific LLC).

the template Tp SOR homodimer contains no metal, and we did not attempt to insert a metal in this domain of the Td SOR model. As shown in Figure 10, the modeled N-terminal domain contains two symmetry-related tetracysteine clusters, each consisting of C10, -23, -30, and -31. Three of the four, C10, -30, and -31, in each cluster reside within one subunit and are homologous to canonical Center I Cys ligand in 2Fe-SORs (cf. Figure 2). The fourth Cys residue, C23, is contributed by the other subunit and is one of the two noncanonical Cys residues, which are yellow-highlighted in Figure 2. The intersubunit Cys residue proximity is particularly evident in one of the modeled tetracysteine clusters, which contains a disulfide bond linking C23 from subunit A with C31 from subunit B. The other noncanonical Cys residue, C22 (also yellow-highlighted in Figure 2), is rotated away from the nearer tetracysteine cluster. As shown in Figure 2, another treponemal SOR sequence, from *T. phagedenis* (Tph), contains the four Cys residues homologous to those of the tetracysteine cluster in the Td SOR model, whereas C22 is substituted by an alanine. The analogous modeling exercise using the Tph SOR sequence resulted in a structure (not shown) that recapitulated the intersubunit tetracysteine clusters (as well as the SOR sites) observed in the Td SOR model. These models are fully

consistent with the Center I Cys ligand residues implicated in our experimental results.

We also generated a Td SOR structural model using a “canonical” 2Fe-SOR template. In this case the SWISS-MODEL server was specifically instructed to use the Db 2Fe-SOR structure shown in Figure 1 as template. The resulting Td SOR model closely resembled the Db 2Fe-SOR structure and showed intrasubunit tricysteine clusters of C10, -30, and -31 superimposed on the corresponding Center I Cys ligands (see Figure S5 in the Supporting Information). However, the noncanonical C22 and C23 in each of the subunits were located ~12 Å away from the nearer tricysteine cluster. This modeling exercise, thus, suggests that C23 ligation in Td SOR Center I cannot be accommodated in the canonical 2Fe-SOR structural motif but *can* be accommodated in the Tp SOR structural motif despite the fact that Tp SOR lacks Center I. We suggest two alternative possibilities for [Fe(Cys)₄] ligation in Td SOR. One is that shown in Figure 10, namely, intrasubunit C10, C30, and C31 and intersubunit C23. Alternatively, intrasubunit ligation of all four Cys ligands may be accommodated in a structure entirely different from those of all other characterized SORs. Either alternative would be unprecedented.

Function(s) of Td SOR in Vivo. The increased air sensitivity of the *T. denticola* SOR gene deletion strain is consistent with an oxidative stress protection role for Td SOR. The even greater sensitivity of the deletion strain to air + MV supports Td SOR's role as a reductive superoxide scavenger. While this role is not unexpected, there appear to be no previous reports of an SOR gene deletion phenotype in any spirochete. The Td SOR active site shows the spectral, redox, and superoxide reactivities characteristic of SORs.

On the other hand, the Cys ligation pattern in Td SOR Center I is novel and could conceivably endow the [Fe(Cys)₄] site with a unique function. Our results do not support a catalytically competent intramolecular electron transfer role for Center I to the SOR site. Reduction of either iron center in Td SOR by the enzymatic system requires Rd, presumably functioning as proximal electron donor. Others have shown that both SOR and Rd transcripts are induced when *T. denticola* is exposed to air.²⁴ On the basis of the two preceding observations, it seems unlikely to us that the Td SOR Center I functions in intermolecular electron transfer to the SOR site in vivo, as has been proposed for Db 2Fe-SOR.³⁷ There appears to be no allosteric effect of Td SOR Center I iron occupancy on reaction of the SOR site with superoxide.

All other 2Fe-SORs reported up to now have been isolated with Center I fully occupied by iron, whereas the as-isolated recombinant Td SOR contained only a small percentage of iron in Center I. We found that, in the presence of a disulfide reducing agent, iron could be quantitatively loaded into Td SOR Center I, resulting in a stable [Fe(Cys)₄] site. A clear implication is that the apo Center I contains a disulfide which hinders iron incorporation. The extent of iron occupancy in Td SOR Center I in vivo could, therefore, reflect both the intracellular dithiol/disulfide redox status and iron flux, particularly during periods of oxidative stress.

Finally, as noted in the Introduction, N-terminal domains of several other uncharacterized Class III SORs contain multiple Cys residues but are not annotated to contain any metal binding motifs.¹² Our results on Td SOR raise the possibility that at least some of these other SORs can accommodate novel Cys-ligated iron sites.

■ ASSOCIATED CONTENT

§ Supporting Information

Depiction of Td SOR homology structural model using the Db SOR structure as template, pKD6H plasmid map; TDE1754 insertional inactivation protocol, Western blot of Td SOR wild type and 1754M cell extracts, primers, and protocol used to construct Cys → Ser variant plasmids. This material is available free of charge via the Internet at <http://pubs.acs.org>.

■ AUTHOR INFORMATION

Corresponding Author

*Tel 210-458-7060; Fax 210-458-7428; e-mail donald.kurtz@utsa.edu.

Funding

This work was supported by the National Institute of Health (D.M.K., Jr., GM040388).

Notes

The authors declare no competing financial interest.

■ ABBREVIATIONS

SOR, superoxide reductase; SOD, superoxide dismutase; SOR site, the [Fe(His)₄Cys] active site characteristic of SORs; Center I, [Fe(Cys)₄] site in 2Fe-SORs; Db, *Desulfoarculatas baarsii*; Tp, *Treponema pallidum*; Td, *Treponema denticola*; Tph, *Treponema phagedenis*; NOS, new oral spirochete medium; MOPS, 3-(N-morpholino)propanesulfonic acid; 1754M, *T. denticola* 35405 strain containing the insertionally inactivated TDE1754 gene; MV, methyl viologen; CFU/mL, colony forming units per mL of culture; TCEP, tris(2-carboxyethyl)-phosphine; DTPA, diethylenetriaminepentaacetic acid; NCBI, National Center for Biotechnology Information (<http://www.ncbi.nlm.nih.gov>); Rd, rubredoxin; NROR, NADH:rubredoxin oxidoreductase.

■ ADDITIONAL NOTES

^aAn archaeal SOR has been reported to assemble a [4Fe–4S] cluster upon addition of iron and sulfide to the as-isolated protein.¹⁷ This SOR contains neither a recognizable Center I domain nor a Cys sequence motif homologous to that of any other SOR class, including any of the Class III SORs.

^bThe 600 nm intermediate in some 1Fe- and 2Fe-SORs undergoes a biphasic decay, which has been attributed to $k_3 < k_2$ in Scheme 1.^{4,7,37}

■ REFERENCES

- (1) Kurtz, D. M., Jr. (2004) Microbial detoxification of superoxide: The non-heme iron reductive paradigm for combating oxidative stress. *Acc. Chem. Res.* 37, 902–908.
- (2) Kurtz, D. M., Jr. (2006) Avoiding high-valent iron intermediates: Superoxide reductase and rubrerythrin. *J. Inorg. Biochem.* 100, 679–693.
- (3) Dermoun, Z., Foulon, A., Miller, M. D., Harrington, D. J., Deacon, A. M., Sebban-Kreuzer, C., Roche, P., Lafitte, D., Bornet, O., Wilson, I. A., and Dolla, A. (2010) TM0486 from the hyperthermophilic anaerobe *Thermotoga maritima* is a thiamin-binding protein involved in response of the cell to oxidative conditions. *J. Mol. Biol.* 400, 463–476.
- (4) Pinto, A. F., Rodrigues, J. V., and Teixeira, M. (2010) Reductive elimination of superoxide: Structure and mechanism of superoxide reductases. *Biochim. Biophys. Acta* 1804, 285–297.
- (5) Jenney, F. E., Jr., Verhagen, M. F. J. M., Cui, X., and Adams, M. W. W. (1999) Anaerobic microbes: oxygen detoxification without superoxide dismutase. *Science* 286, 306–309.

- (6) Huang, V. W., Emerson, J. P., and Kurtz, D. M., Jr. (2007) Reaction of *Desulfovibrio vulgaris* two-iron superoxide reductase with superoxide: Insights from stopped-flow spectrophotometry. *Biochemistry* 46, 11342–11351.
- (7) Bonnot, F., Houee-Levin, C., Favaudon, V., and Niviere, V. (2010) Photochemical processes observed during the reaction of superoxide reductase from *Desulfoarculus baarsii* with superoxide: Re-evaluation of the reaction mechanism. *Biochim. Biophys. Acta* 1804, 762–767.
- (8) Testa, F., Mastronicola, D., Cabelli, D. E., Bordin, E., Pucillo, L. P., Sarti, P., Saraiva, L. M., Giuffrè, A., and Teixeira, M. (2011) The superoxide reductase from the early diverging eukaryote *Giardia intestinalis*. *Free Radical Biol. Med.* 51, 1567–1574.
- (9) Lombard, M., Fontecave, M., Touati, D., and Nivière, V. (2000) Reaction of the desulfoferrodoxin from *Desulfoarculus baarsii* with superoxide anion. Evidence for a superoxide reductase activity. *J. Biol. Chem.* 275, 115–121.
- (10) Yeh, A. P., Hu, Y., Jenney, F. E., Jr., Adams, M. W., and Rees, D. C. (2000) Structures of the superoxide reductase from *Pyrococcus furiosus* in the oxidized and reduced states. *Biochemistry* 39, 2499–2508.
- (11) Katona, G., Carpentier, P., Niviere, V., Amara, P., Adam, V., Ohana, J., Tsanov, N., and Bourgeois, D. (2007) Raman-assisted crystallography reveals end-on peroxide intermediates in a nonheme iron enzyme. *Science* 316, 449–453.
- (12) Lucchetti-Miganeh, C., Goudenege, D., Thybert, D., Salbert, G., and Barloy-Hubler, F. (2011) SORGOdb: superoxide reductase gene ontology curated dataBase. *BMC Microbiol.* 11, 105.
- (13) Emerson, J. P., Cabelli, D. E., and Kurtz, D. M., Jr. (2003) An engineered two-iron superoxide reductase lacking the [Fe(SCys)₄] site retains its catalytic properties in vitro and in vivo. *Proc. Natl. Acad. Sci. U. S. A.* 100, 3802–3807.
- (14) Lombard, M., Touati, D., Fontecave, M., and Nivière, V. (2000) Superoxide reductase as a unique defense system against superoxide stress in the microaerophile *Treponema pallidum*. *J. Biol. Chem.* 275, 27021–27026.
- (15) Jovanovic, T., Ascenso, C., Hazlett, K. R., Sikkink, R., Krebs, C., Litwiller, R., Benson, L. M., Moura, I., Moura, J. J., Radolf, J. D., Huynh, B. H., Naylor, S., and Rusnak, F. (2000) Neelaredoxin, an iron-binding protein from the syphilis spirochete, *Treponema pallidum*, is a superoxide reductase. *J. Biol. Chem.* 275, 28439–28448.
- (16) Santos-Silva, T., Trincão, J., Carvalho, A. L., Bonifacio, C., Auchere, F., Raleiras, P., Moura, I., Moura, J. J. G., and Romão, M. J. (2006) The first crystal structure of class III superoxide reductase from *Treponema pallidum*. *J. Biol. Inorg. Chem.* 11, 548–558.
- (17) Kratzer, C., Welte, C., Dorner, K., Friedrich, T., and Deppenmeier, U. (2011) Methanoferrodoxin represents a new class of superoxide reductase containing an iron-sulfur cluster. *FEBS J.* 278, 442–451.
- (18) Limberger, R. J., Slivinski, L. L., Izard, J., and Samsonoff, W. A. (1999) Insertional inactivation of *Treponema denticola* *tap1* results in a nonmotile mutant with elongated flagellar hooks. *J. Bacteriol.* 181, 3743–3750.
- (19) Holt, S. C., and Ebersole, J. L. (2005) *Porphyromonas gingivalis*, *Treponema denticola*, and *Tannerella forsythia*: the 'red complex', a prototype polybacterial pathogenic consortium in periodontitis. *Periodontology* 2000 (38), 72–122.
- (20) Dashper, S. G., Seers, C. A., Tan, K. H., and Reynolds, E. C. (2011) Virulence factors of the oral spirochete *Treponema denticola*. *J. Dent. Res.* 90, 691–703.
- (21) Seshadri, R., Myers, G. S., Tettelin, H., Eisen, J. A., Heidelberg, J. F., Dodson, R. J., Davidsen, T. M., DeBoy, R. T., Fouts, D. E., Haft, D. H., Selengut, J., Ren, Q., Brinkac, L. M., Madupu, R., Kolonay, J., Durkin, S. A., Daugherty, S. C., Shetty, J., Shvartsbeyn, A., Gebregeorgis, E., Geer, K., Tsegaye, G., Malek, J., Ayodeji, B., Shatsman, S., McLeod, M. P., Smajls, D., Howell, J. K., Pal, S., Amin, A., Vashisth, P., McNeill, T. Z., Xiang, Q., Sodergren, E., Baca, E., Weinstock, G. M., Norris, S. J., Fraser, C. M., and Paulsen, I. T. (2004) Comparison of the genome of the oral pathogen *Treponema denticola* with other spirochete genomes. *Proc. Natl. Acad. Sci. U. S. A.* 101, 5646–5651.
- (22) Veith, P. D., Dashper, S. G., O'Brien-Simpson, N. M., Paolini, R. A., Orth, R., Walsh, K. A., and Reynolds, E. C. (2009) Major proteins and antigens of *Treponema denticola*. *Biochim. Biophys. Acta* 1794, 1421–1432.
- (23) Parsonage, D., Desrosiers, D. C., Hazlett, K. R. O., Sun, Y. C., Nelson, K. J., Cox, D. L., Radolf, J. D., and Poole, L. B. (2010) Broad specificity AhpC-like peroxiredoxin and its thioredoxin reductant in the sparse antioxidant defense system of *Treponema pallidum*. *Proc. Natl. Acad. Sci. U. S. A.* 107, 6240–6245.
- (24) McHardy, I., Keegan, C., Sim, J. H., Shi, W. Y., and Lux, R. (2010) Transcriptional profiles of *Treponema denticola* in response to environmental conditions. *PLoS One* 5, e13655.
- (25) Lumpio, H. L., Shen, N. V., Summers, A. O., Voordouw, G., and Kurtz, D. M., Jr. (2001) Rubrerythrin and rubredoxin oxidoreductase in *Desulfovibrio vulgaris*. A novel oxidative stress protection system. *J. Bacteriol.* 183, 101–108 and correction 2970.
- (26) Melcher, K. (2000) A modular set of prokaryotic and eukaryotic expression vectors. *Anal. Biochem.* 277, 109–120.
- (27) Melcher, K. (2000) Errata to: A modular set of prokaryotic and eukaryotic expression vectors. *Anal. Biochem.* 282, 266–266.
- (28) Xiong, J., Kurtz, D. M., Jr., Ai, J., and Sanders-Loehr, J. (2000) A hemerythrin-like domain in a bacterial chemotaxis protein. *Biochemistry* 39, 5117–5125.
- (29) Stookey, L. L. (1970) Ferrozine - a new spectrophotometric reagent for iron. *Anal. Chem.* 42, 779–781.
- (30) Hillmann, F., Riebe, O., Fischer, R. J., Mot, A., Caranto, J. D., Kurtz, D. M., Jr., and Bahl, H. (2009) Reductive dioxygen scavenging by flavo-diiron proteins of *Clostridium acetobutylicum*. *FEBS Lett.* 583, 241–245.
- (31) Coulter, E. D., and Kurtz, D. M., Jr. (2001) A role for rubredoxin in oxidative stress protection in *Desulfovibrio vulgaris*: catalytic electron transfer to rubrerythrin and two-iron superoxide reductase. *Arch. Biochem. Biophys.* 394, 76–86.
- (32) Clay, M. D., Jenney, F. E., Jr., Hagedoorn, P. L., George, G. N., Adams, M. W. W., and Johnson, M. K. (2002) Spectroscopic studies of *Pyrococcus furiosus* superoxide reductase: implications for active-site structures and the catalytic mechanism. *J. Am. Chem. Soc.* 124, 788–805.
- (33) Emerson, J. P., Coulter, E. D., Cabelli, D. E., Phillips, R. S., and Kurtz, D. M., Jr. (2002) Kinetics and mechanism of superoxide reduction by two-iron superoxide reductase from *Desulfovibrio vulgaris*. *Biochemistry* 41, 4348–4357.
- (34) Xiao, Z., Lavery, M. J., Ayhan, M., Scrofan, S. D. B., Wilce, M. C. J., Guss, J. M., Tregloan, P. A., George, G. N., and Wedd, A. G. (1998) The rubredoxin from *Clostridium pasteurianum*: mutation of the iron cysteinyl ligands to serine. Crystal and molecular structures of oxidized and dithionite-treated forms of the Cys42Ser mutant. *J. Am. Chem. Soc.* 120, 4135–4150.
- (35) Xiao, Z., Gardner, A. R., Cross, M., Maes, E. M., Czernuszewicz, R. S., Sola, M., and Wedd, A. G. (2001) Redox thermodynamics of mutant forms of the rubredoxin from *Clostridium pasteurianum*: identification of a stable FeIII(S-Cys)₃(OH) centre in the C6S mutant. *J. Biol. Inorg. Chem.* 6, 638–649.
- (36) Morleo, A., Bonomi, F., Iametti, S., Huang, V. W., and Kurtz, D. M., Jr. (2010) Iron-nucleated folding of a metalloprotein in high urea: resolution of metal binding and protein folding events. *Biochemistry* 49, 6627–6634.
- (37) Bonnot, F., Duval, S., Lombard, M., Valton, J., Houee-Levin, C., and Niviere, V. (2011) Intermolecular electron transfer in two-iron superoxide reductase: a putative role for the desulfoferrodoxin center as an electron donor to the iron active site. *J. Biol. Inorg. Chem.* 16, 889–898.
- (38) Emerson, J. P., Coulter, E. D., Phillips, R. S., and Kurtz, D. M., Jr. (2003) Kinetics of the superoxide reductase catalytic cycle. *J. Biol. Chem.* 278, 39662–39668.
- (39) Rodrigues, J. V., Abreu, I. A., Saraiva, L. M., and Teixeira, M. (2005) Rubredoxin acts as an electron donor for neelaredoxin in

Archaeoglobus fulgidus. *Biochem. Biophys. Res. Commun.* 329, 1300–1305.

(40) Arnold, K., Bordoli, L., Kopp, J., and Schwede, T. (2006) The SWISS-MODEL workspace: a web-based environment for protein structure homology modelling. *Bioinformatics* 22, 195–201.